Molecule formation as a diagnostic tool for second-order correlations of ultracold gases

D. Meiser and P. Meystre
Optical Sciences Center, The University of Arizona, Tucson, Arizona 85721, USA

C. P. Search
Department of Physics and Engineering Physics, Stevens Institute of Technology, Hoboken, New Jersey 07030, USA
(Received 11 December 2004; published 21 March 2005)

We calculate the momentum distribution and the second-order correlation function in momentum space, $g^{(2)}(\mathbf{p},\mathbf{p}',t)$ for molecular dimers that are coherently formed from an ultracold atomic gas by photoassociation or a Feshbach resonance. We investigate using perturbation theory how the quantum statistics of the molecules depend on the initial state of the atoms by considering three different initial states: a Bose-Einstein condensate (BEC), a normal Fermi gas of ultracold atoms, and a BCS-type superfluid Fermi gas. The cases of strong and weak coupling to the molecular field are discussed. It is found that BEC and BCS states give rise to an essentially coherent molecular field with a momentum distribution determined by the zero-point motion in the confining potential. On the other hand, a normal Fermi gas and the unpaired atoms in the BCS state give rise to a molecular field with a broad momentum distribution and thermal number statistics. It is shown that the first-order correlations of the molecules can be used to measure second-order correlations of the initial atomic state.

DOI: 10.1103/PhysRevA.71.033621 PACS number(s): 03.75.Hh, 39.20.+q, 74.90.+n

I. INTRODUCTION

The basis of some of the most exciting developments in ultracold atomic physics in recent years has been the use of Feshbach resonances [1,2] and photoassociation [3,4] to tune the strength of the interactions between atoms as well as to create ultracold diatomic molecules starting from an ultracold atomic gas of bosons or fermions [1,5–10]. The availability of tunable interactions has made possible the study of many model systems of condensed-matter theory in a very controlled fashion [11–16]. In particular, the BEC-BCS crossover, which predicts a continuous transition from a BCS superfluid of atomic fermions to a molecular BEC as the interaction strength is varied from attractive to repulsive, has attracted a considerable amount of attention, both experimentally and theoretically [16–21].

A difficulty in the studies of the BEC-BCS crossover has been that they necessitate the measurement of higher-order correlations of the atomic system. While the momentum distribution of a gas of bosons provides a clear signature of the presence of a Bose-Einstein condensate, the Cooper pairing between Fermionic atoms in a BCS state hardly changes the momentum distribution or spatial profile as compared to a normal Fermi gas. This poses a significant experimental challenge, since the primary techniques for probing the state of an ultracold gas are either optical absorption or phase contrast imaging, which directly measure the spatial density or momentum distribution following ballistic expansion of the gas. In the strongly interacting regime very close to the Feshbach resonance, evidence for Fermionic superfluidity was obtained by projecting the atom pairs onto a molecular state by a rapid sweep through the resonance [17,19]. More direct evidence of the gap in the excitation spectra due to pairing was obtained by rf spectroscopy [22] and by measurements of the collective excitation frequencies [23,24].

Still, the detection of Fermionic superfluidity in the weakly interacting BCS regime remains a challenge. The direct detection of Cooper pairing requires the measurement of second-order or higher atomic correlation functions. Several researchers have proposed and implemented schemes that allow one to measure higher-order correlations [17,25–29] but those methods are still very difficult to realize experimentally.

While the measurement of higher-order correlations is challenging already for bosons, the theory of these correlations has been established a long time ago by Glauber for photons [30–32]. For fermions however, despite some efforts [33] a satisfactory coherence *theory* is still missing.

To circumvent these difficulties we suggested in an earlier publication [34], guided by the analogy with three-wave mixing in classical optics, to make use of the nonlinear coupling of atoms to a molecular field by means of a two-photon Raman transition or a Feshbach resonance. The nonlinearity of the coupling links first-order correlations of the molecules to second-order correlations of the atoms. Furthermore, the molecules are always Bosonic so that the well-known coherence theory for Bosonic fields can be used to characterize them. Considering a simplified model with only one molecular mode, it was found that the molecules created that way can indeed be used as a diagnostic tool for second-order correlations of the original atomic field. Naturally, due to the restriction to a single mode, the information one can gain about the atomic state is very limited.

In this paper we extend the previous model to take into account all modes of the molecular field, the hope being that in doing so, more detailed information about the atomic state can be obtained. Specifically, we calculate the momentum distribution of the molecules and the normalized second-order correlation function, $g^{(2)}$ for different momentum states of the molecules using perturbation theory. We consider the limiting cases of strong or weak atom molecule coupling as compared to the relevant atomic energies. The molecule formation from a Bose-Einstein condensate (BEC) serves as a

reference system. There we can rather easily study the contributions to the molecular signal from the condensed fraction as well as from thermal and quantum fluctuations above the condensate. The cases of a normal Fermi gas and a BCS superfluid Fermi system are then compared with it. We show that the molecule formation from a normal Fermi gas and from the unpaired fraction of atoms in a BCS state has very similar properties to those of the molecules formed from the noncondensed atoms in the BEC case. The state of the molecular field formed from the pairing field in the BCS state on the other hand is similar to that resulting from the condensed fraction in the BEC case. The qualitative information gained by the analogies with the BEC case help us gain a physical understanding of the molecule formation in the BCS case where direct calculations are difficult and not nearly as transparent.

This paper is organized as follows: In Sec. II we introduce the model Hamiltonian used to describe the coupled atom-molecule system. In secs. III–V we present the calculations of momentum distribution and second factorial moment of the molecular field for a BEC, a normal Fermi gas, and a BCS-type state, respectively, considering the cases of strong and weak coupling in each case. Details of the calculations are given in Appendixes A and B.

II. MODEL

The general procedure that we have in mind is the following: The atomic sample is prepared in some initial state, whose higher-order correlations we seek to analyze. At time $t=0$ the coupling to a molecular field is switched on. While the initial atomic state corresponds to a trapped gas, we assume that the molecules can be treated as free particles. This is justified if the atomic trapping potential does not affect the molecules, or if the interaction time between the atoms and molecules is much less than the oscillation period in the trap. Finally, the state of the molecular field is analyzed by standard techniques, e.g., time-of-flight measurements.

We consider the three cases where the atoms are Bosonic and initially form a BEC, or consist of two species of ultracold fermions (labeled by $\sigma=\uparrow,\downarrow$), with or without superfluid component. In the following we describe explicitly the situation for fermions, the Bosonic case being obtained from it by omitting the spin indices and by replacing the Fermi field operators by Bosonic field operators.

Since we are primarily interested in how much can be learned about the second-order correlations of the initial atomic cloud from the final molecular state, we keep the physics of the atoms themselves as well as the coupling to the molecular field as simple as possible. The coupled fermion-molecule system can be described by the Hamiltonian [2,35,36]

$$\hat{H} = \sum_{\mathbf{k},\sigma} \epsilon_{\mathbf{k}} \hat{c}^{\dagger}_{\mathbf{k}\sigma}\hat{c}_{\mathbf{k}\sigma} + \sum_{\mathbf{k}} E_{\mathbf{k}} \hat{a}^{\dagger}_{\mathbf{k}}\hat{a}_{\mathbf{k}} + V^{-1/2} \sum_{\mathbf{k}_1,\mathbf{k}_2,\sigma} \tilde{U}_{\mathrm{tr}}(\mathbf{k}_2 - \mathbf{k}_1)\hat{c}^{\dagger}_{\mathbf{k}_2\sigma}\hat{c}_{\mathbf{k}_1\sigma} + \frac{U_0}{2V} \sum_{\mathbf{q},\mathbf{k}_1,\mathbf{k}_2} \hat{c}^{\dagger}_{\mathbf{k}_1+\mathbf{q}\uparrow}\hat{c}^{\dagger}_{\mathbf{k}_2-\mathbf{q}\downarrow}\hat{c}_{\mathbf{k}_2\downarrow}\hat{c}_{\mathbf{k}_1\uparrow} + g\left(\sum_{\mathbf{q},\mathbf{k}} \hat{a}^{\dagger}_{\mathbf{q}}\hat{c}_{\mathbf{q}/2+\mathbf{k}\downarrow}\hat{c}_{\mathbf{q}/2-\mathbf{k}\uparrow} + \mathrm{H.c.}\right) \quad (1)$$

Here $\epsilon_{\mathbf{k}}=k^2/2M$ is the kinetic energy of an atom of mass M and momentum $\mathbf{k}$ and $E_{\mathbf{k}}=\epsilon_{\mathbf{k}}/2+\nu$ is the energy of a molecule with momentum k and detuning parameter ν. $c_{\mathbf{k}\sigma}$ and $c^{\dagger}_{\mathbf{k}\sigma}$ are Fermionic annihilation and creation operators for plain waves in quantization volume V with spin σ. $\tilde{U}_{\mathrm{tr}}(\mathbf{k}) = V^{-1/2}\int_V d^3x e^{-i\mathbf{k}\cdot\mathbf{x}} U_{\mathrm{tr}}(\mathbf{x})$ is the Fourier transform of the trapping potential $U_{\mathrm{tr}}(\mathbf{r})$ and $U_0=4\pi a/M$ is the background scattering strength, g is the effective coupling constant of the atoms to the molecules, and we use units with $\hbar\equiv 1$ throughout. We assume that the trapping potential and background scattering are relevant only for the preparation of the initial state before the coupling to the molecules is switched on at $t=0$ and can be neglected in the calculation of the dynamics. This is justified if $g\sqrt{N}\gg U_0 n,\ \omega_i$ where n is the atomic density, N the number of atoms, and ω_i are the frequencies of $U_{\mathrm{tr}}(\mathbf{r})$ that is assumed to be harmonic. In experiments, the interaction between the atoms can effectively be switched off by ramping the magnetic field to a position where the scattering length is zero.

Regarding the strength of the coupling constant g, two cases are possible: $g\sqrt{N}$ can be much larger or much smaller than the characteristic kinetic energies involved. For fermions the terms broad and narrow resonance have been coined for the two cases, respectively, and we will use these for bosons as well. Both situations can be realized experimentally, and they give rise to different effects. We examine both limiting cases and use the suggestive notation $E_{\mathrm{kin}}\ll g\sqrt{N}$ and $E_{\mathrm{kin}}\gg g\sqrt{N}$ for the two cases, where E_{kin} denotes the characteristic kinetic energy of the atoms. It corresponds to zero point motion for condensate atoms, to the thermal energy, k_BT for noncondensed thermal bosons, and to the Fermi energy for a degenerate Fermi gas.

Our analysis is based on the assumption that first-order time-dependent perturbation theory is applicable. This requires that the state of the atoms does not change significantly and consequently, only a small fraction of the atoms are converted into molecules. It is reasonable to assume that this is true for short interaction times or weak enough coupling. Apart from making the system tractable by analytic methods there is also a deeper reason why the coupling should be weak: Since we ultimately wish to get information about the atomic state, it should not be modified too much by the measurement itself, i.e., the coupling to the molecular field. Our treatment therefore follows the same spirit as Glauber's original theory of photon detection, where it is assumed that the light-matter coupling is weak enough that the detector photocurrent can be calculated using Fermi's golden rule.

III. BEC

We consider first the case where the initial atomic state is a BEC in a spherically symmetric harmonic trap. We note that all of our results can readily be extended to anisotropic traps by an appropriate rescaling of the coordinates in the direction of the trap axes. We assume that the temperature is well below the BEC transition temperature and that the interactions between the atoms are not too strong. Then the

atomic system is described by the field operator

$$\hat{\psi}(\mathbf{x}) = \chi_0(\mathbf{x})\hat{c} + \delta\hat{\psi}(\mathbf{x}), \tag{2}$$

where

$$\chi_0(\mathbf{x}) = \sqrt{\frac{15}{8\pi R_{\mathrm{TF}}^3}}\sqrt{1-\frac{x^2}{R_{\mathrm{TF}}^2}} \tag{3}$$

is the condensate wave function in the Thomas-Fermi approximation and $\hat{c}$ is the annihilation operator for an atom in the condensate, $R_{\mathrm{TF}}=(15Na/a_{\mathrm{osc}})^{1/5}a_{\mathrm{osc}}$ is the Thomas-Fermi radius, N the number of atoms, a is their scattering length, and a_{osc} is the oscillator length of the atoms in the trap. In accordance with the assumption of low temperatures and weak interactions we do not distinguish between the total number of atoms and the number of atoms in the condensate. The fluctuations $\delta\hat{\psi}(\mathbf{x})$ are small and those with wavelengths much less than R_{TF} will be treated in the local-density approximation while those with wavelengths comparable to R_{TF} can be neglected [37–39].

A. Broad resonance, $E_{\mathrm{kin}} \ll g\sqrt{N}$

We are interested in the momentum distribution of the molecules

$$n(\mathbf{p},t) = \langle \hat{a}_{\mathbf{p}}^{\dagger}(t)\hat{a}_{\mathbf{p}}(t)\rangle \tag{4}$$

which for short times t can be calculated using perturbation theory: We expand $n(\mathbf{p},t)$ in a Taylor series around $t=0$ and make use of the Heisenberg equations of motion,

$$i\frac{\partial \hat{a}_{\mathbf{p}}(t)}{\partial t} = g\sum_{\mathbf{k}} \hat{c}_{\mathbf{p}/2+\mathbf{k}}\hat{c}_{\mathbf{p}/2-\mathbf{k}}, \tag{5}$$

and similarly for $\hat{a}_{\mathbf{p}}^{\dagger}$. Here we have neglected the kinetic energy term, a step that is legitimate for a broad resonance since the interaction energy $g\sqrt{N}$ is much larger than the difference in the kinetic energies between the atoms and molecules. Consequently for short enough times, $t \lesssim (g\sqrt{N})^{-1}$, energy conservation can be violated in the formation of molecules in a fashion similar to the Raman-Nath regime of atomic diffraction.

To lowest nonvanishing order in gt we find

$$n_{\mathrm{BEC},b}(\mathbf{p},t) = (gt)^2 \sum_{\mathbf{k}_1,\mathbf{k}_2} \langle \hat{c}_{\mathbf{p}/2-\mathbf{k}_1}^{\dagger}\hat{c}_{\mathbf{p}/2+\mathbf{k}_1}^{\dagger}\hat{c}_{\mathbf{p}/2+\mathbf{k}_2}\hat{c}_{\mathbf{p}/2-\mathbf{k}_2}\rangle + \mathcal{O}[(gt)^4], \tag{6}$$

where the atomic operators are the initial ($t=0$) operators. This expression can be evaluated by making use of the decomposition of the atomic field operator (2) and the local-density approximation for the part describing the fluctuations. The details of this calculation are given in Appendix A. To first nonvanishing order in the fluctuations we find

$$n_{\mathrm{BEC},b}(\mathbf{p},t) = (gt)^2 N(N-1)V|\tilde{\chi}_0^2(\mathbf{p})|^2 + (gt)^2 4N\int \frac{d^3x}{V}\langle \delta\hat{c}_{\mathbf{p}}^{\dagger}(\mathbf{x})\delta\hat{c}_{\mathbf{p}}(\mathbf{x})\rangle. \tag{7}$$

From this expression we see that our approach is justified if $(\sqrt{N}gt)^2 \ll 1$ because for such times the initial atomic state can be assumed to remain undepleted.

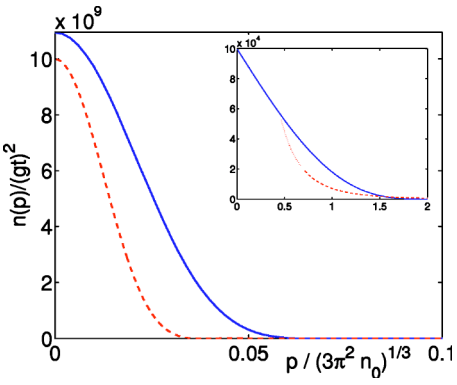

FIG. 1. (Color online) Momentum distribution of molecules formed from a BEC (red dashed line) with $a=0.1a_{\mathrm{osc}}$ and $T=0.1T_c$ and a BCS-type state with $k_Fa=0.5$ and $a_{\mathrm{osc}}=5k_F^{-1}(0)$ (blue solid line), both for $N=10^5$ atoms. The BCS curve has been scaled up by a factor of 20 for easier comparison. The inset shows the noise contribution for BEC (red dashed) and BCS (blue) case. The latter is simply the momentum distribution of molecules formed from a normal Fermi gas. The local-density approximation treatment of the noise contribution in the BEC case is not valid for momenta smaller than $2\pi/\xi$ (indicated by the red dotted line in the inset). Note that the coherent contribution is larger than the noise contribution by five orders of magnitude in the BEC case and three orders of magnitude in the BCS case.

In the local-density approximation the expectation value $\langle \delta\hat{c}_{\mathbf{p}}^{\dagger}(\mathbf{x})\delta\hat{c}_{\mathbf{p}}(\mathbf{x})\rangle$ for the number of fluctuations with momentum $\mathbf{p}$ at $\mathbf{x}$ can be evaluated by assuming that at each $\mathbf{x}$ we have a homogenous BEC with density $n(\mathbf{x})$ and using the Bogoliubov transformation to quasiparticle operators, $\hat{\alpha}_{\mathbf{k}}(\mathbf{x})$. One finds

$$\langle \delta\hat{c}_{\mathbf{p}}^{\dagger}(\mathbf{x})\delta\hat{c}_{\mathbf{p}}(\mathbf{x})\rangle = v_{\mathbf{p}}^2(\mathbf{x}) + [u_{\mathbf{p}}^2(\mathbf{x}) + v_{\mathbf{p}}^2(\mathbf{x})]\langle \hat{\alpha}_{\mathbf{p}}^{\dagger}(\mathbf{x})\hat{\alpha}_{\mathbf{p}}(\mathbf{x})\rangle, \tag{8}$$

with Bogoliubov amplitudes

$$u_{\mathbf{p}}^2(\mathbf{x}) = \frac{1}{2}\left[\frac{\frac{p^2}{2M}+n(\mathbf{x})U_0}{\tilde{\epsilon}_{\mathbf{p}}(\mathbf{x})}+1\right], \tag{9}$$

$$v_{\mathbf{p}}^2(\mathbf{x}) = \frac{1}{2}\left[\frac{\frac{p^2}{2M}+n(\mathbf{x})U_0}{\tilde{\epsilon}_{\mathbf{p}}(\mathbf{x})}-1\right], \tag{10}$$

and quasiparticle energies

$$\tilde{\epsilon}_{\mathbf{p}}(\mathbf{x}) = \sqrt{\epsilon_{\mathbf{p}}^2 + 2\epsilon_{\mathbf{p}}n(\mathbf{x})U_0}. \tag{11}$$

The quasiparticle distribution is given by a thermal Bose distribution,

$$\langle \hat{\alpha}_{\mathbf{p}}^{\dagger}(\mathbf{x})\hat{\alpha}_{\mathbf{p}}(\mathbf{x})\rangle = \frac{1}{e^{\tilde{\epsilon}_{\mathbf{p}}(\mathbf{x})/k_BT}-1}. \tag{12}$$

The momentum distribution (7) is illustrated in Fig. 1. The contribution from the condensate is a collective effect,

as indicated by its quadratic scaling with the atom number. It clearly dominates over the incoherent contribution from the fluctuations, which is proportional to the number of atoms. The momentum width of the contribution from the condensate is roughly $2\pi/R_{\mathrm{TF}}$ which is much narrower than the contribution from the fluctuations, whose momentum distribution has a typical width of $1/\xi$, where $\xi=(8\pi an)^{-1/2}$ is the healing length. Using the Thomas-Fermi wave function for the condensate, Eq. (3), we can calculate the condensate contribution in closed form as

$$n_{\mathrm{BEC},b}(\mathbf{p},t)=\frac{225N(N-1)(gt)^2}{4(pR_{TF})^6}\left(\frac{6\sin pR_{TF}}{(pR_{TF})^2}-\frac{6\cos pR_{TF}}{pR_{TF}}-2\sin pR_{TF}\right)^2+\mathcal{O}(N). \tag{13}$$

The terms of order N are corrections due to the noncondensed part.

Using the same approximation scheme we can calculate the second-order correlation,

$$g^{(2)}(\mathbf{p}_1,t_1;\mathbf{p}_2,t_2)=\frac{\langle\hat{a}^\dagger_{\mathbf{p}_1}(t_1)\hat{a}^\dagger_{\mathbf{p}_2}(t_2)\hat{a}_{\mathbf{p}_2}(t_2)\hat{a}_{\mathbf{p}_1}(t_1)}{n(\mathbf{p}_1,t_1)n(\mathbf{p}_2,t_2)}. \tag{14}$$

If we neglect fluctuations we find

$$g^{(2)}_{\mathrm{BEC},b}(\mathbf{p}_1,t_1;\mathbf{p}_2,t_2)=\frac{(N-2)!^2}{(N-4)!\,N!}=1-\frac{6}{N}+\mathcal{O}(N^{-2}). \tag{15}$$

For $N\to\infty$ this is very close to 1, which is characteristic of a coherent state. This result implies that the number fluctuations of the molecules are very nearly Poissonian. The fluctuations lead to a larger value of $g^{(2)}$, making the molecular field partially coherent, but their effect is only of order $\mathcal{O}(N^{-1})$.

The physical reason why the resulting molecular field is almost coherent is of course clear: The condensed fraction of the atomic field operator is dominant. In expectation values the operators $\hat{c}$ and $\hat{c}^\dagger$ take on values $\sqrt{N-n}$, with a number $n\ll N$ depending on the position of the operator in the expectation value. When dividing by the normalizing expectation values $n(\mathbf{p},t)$, $\sqrt{N-n}$ can be replaced by $\sqrt{N}$ with accuracy $\mathcal{O}(N^{-1})$ and hence $\hat{c}$ and $\hat{c}^\dagger$ can be replaced by $\sqrt{N}$ independent of their position in the expectation value. The field operator can thus be replaced by a c-number field $\hat{\psi}(x)\to\sqrt{N}\chi_0(x)$, the mean field, which explains the almost perfect factorization of the correlation functions.

Another way to understand this is to consider the single-mode BEC state, $|\Psi(0)\rangle=(\hat{c}^\dagger\hat{c}^\dagger)^{(N/2)}|0\rangle/\sqrt{N!}$. The coupling to the molecular field will transform this state into $|\Psi(t)\rangle\approx(\alpha\hat{a}^\dagger+\beta\hat{c}^\dagger\hat{c}^\dagger)^{(N/2)}|0\rangle/\sqrt{N!}$, where $\alpha\ll1$. This leads to a binomial distribution for the number of molecules. In the limit that $N\to\infty$ the Binomial distribution goes over to the Poisson distribution.

B. Narrow resonance, $E_{\mathrm{kin}}\gg g\sqrt{N}$

For a narrow resonance, the typical kinetic energies associated with the atoms and molecules, E_{kin}, are much larger than the atom-molecule interaction energy. This implies that even for very short interaction times, $t\lesssim(g\sqrt{N})^{-1}$, the phase of the atoms and molecules can evolve significantly, $E_{\mathrm{kin}}t\gg1$. Consequently, only transitions between atom pairs and molecules that conserve energy can occur. In this case, it is convenient to go over to the interaction representation,

$$\hat{c}_{\mathbf{p}}(t)\to e^{-i\epsilon_{\mathbf{p}}t}\hat{c}_{\mathbf{p}}(t),\quad \hat{a}_{\mathbf{p}}(t)\to e^{-iE_{\mathbf{p}}t}\hat{a}_{\mathbf{p}}(t), \tag{16}$$

where for notational convenience, we will denote the interaction picture operators by the same symbols as the Heisenberg operators used in the previous subsection.

The equations of motion in the interaction picture,

$$i\frac{\partial\hat{a}_{\mathbf{p}}(t)}{\partial t}=g\sum_{\mathbf{k}}e^{i(E_{\mathbf{p}}-\epsilon_{\mathbf{p}/2+\mathbf{k}}-\epsilon_{\mathbf{p}/2-\mathbf{k}})t}\hat{c}_{\mathbf{p}/2+\mathbf{k}}\hat{c}_{\mathbf{p}/2-\mathbf{k}}, \tag{17}$$

can be approximately integrated by treating the atomic operators as constants, leading to

$$\hat{a}_{\mathbf{p}}(t)=\sum_{\mathbf{k}}\Delta(E_p-\epsilon_{\mathbf{p}/2+\mathbf{k}}-\epsilon_{\mathbf{p}/2-\mathbf{k}},t)\hat{c}_{\mathbf{p}/2+\mathbf{k}}\hat{c}_{\mathbf{p}/2-\mathbf{k}}, \tag{18}$$

where we have introduced[1]

$$\Delta(\omega,t)=g\lim_{\eta\downarrow0}\frac{e^{i\omega t}-1}{i\omega+\eta}. \tag{19}$$

The condition under which this step is justified is analyzed below. As in the broad resonance case we can insert this expression in $n(\mathbf{p},t)$. The calculation of the resulting integrals over expectation values of the atomic state is, however, considerably subtler than in the broad resonance case and is presented in detail in Appendix B. In the limit $\nu t\gg1$ we find

$$\begin{aligned}n_{\mathrm{BEC},n}(\mathbf{p},t)=N(N-1)\frac{V^2M^3g^2}{16\pi^4}\Bigg|\int_0^\infty d\omega\sqrt{\omega}\Bigg(\pi\delta(\nu-\omega)&\\+i\mathbf{P}\frac{1}{\nu-\omega}\Bigg)\int_{-1}^1dz\tilde{\chi}_0(\sqrt{p^2/4+M\omega-p\sqrt{M\omega}z})&\\\times\tilde{\chi}_0(\sqrt{p^2/4+M\omega+p\sqrt{M\omega}z})\Bigg|^2&\\+N\delta_{p/2,\sqrt{M\nu}}\frac{3g^2t\sqrt{\nu M^3}R_{TF}^3}{8\pi^2}&\\\times\int\frac{d^3x}{V}\langle\delta\hat{c}^\dagger_{\mathbf{p}}(\mathbf{x})\delta\hat{c}_{\mathbf{p}}(\mathbf{x})\rangle.&\end{aligned} \tag{20}$$

In the second term in Eq. (20) we have defined

[1]We denote the function in Eq. (19) by Δ because it has properties similar to the usual δ function. Confusion with the local gap parameter introduced below, which we also denote by Δ, cannot arise because the first always has energies as its argument while the latter has positions as its argument.

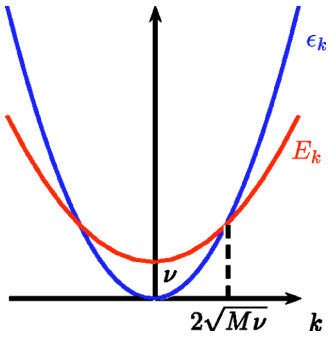

FIG. 2. (Color online) In the narrow resonance case for momenta p much larger than the momentum width of the condensate one atom is taken out of the condensate and the other atom is taken from the noncondensed part and has momentum close to p in order for momentum conservation to be satisfied. Since the total energy of the atoms has to match the total energy of the molecule, only molecules with momenta $2\sqrt{M\nu}$ can be formed for each detuning ν.

$$\delta_{p,p'} = \sqrt{\frac{4\pi V}{3R_{TF}^3}}\int_{-1}^{1} dz|\tilde{\chi}_0(\sqrt{p^2+p'^2-2pp'z})|^2 = \begin{cases} \mathcal{O}(1), & |p-p'| < 2\pi/R_{\mathrm{TF}} \\ 0, & |p-p'| > 2\pi/R_{\mathrm{TF}}. \end{cases} \tag{21}$$

As before, the contribution from the condensate is clearly dominant. The integral in the first term in Eq. (20) is proportional to the amplitude for finding an atom pair with center of mass momentum $\mathbf{p}$ and total kinetic energy ν. Because $\tilde{\chi}_0$ drops to zero on a scale of $2\pi/R_{TF}$ this amplitude is essentially zero if $p > 2\pi/R_{\mathrm{TF}}$ or $\nu > \pi^2/MR_{\mathrm{TF}}^2$.

The second term in Eq. (20) originates from molecules that are formed from an atom in the condensate and a noncondensed atom. Since the atom momentum $\lesssim 2\pi/R_{\mathrm{TF}}$ in the condensate is very small compared to the momentum $|\mathbf{p}| \sim 1/\xi$ of a noncondensed atom, the molecular momentum is essentially due to the noncondensed atom. On the other hand, energy conservation implies that $\nu + p^2/4M \approx p^2/2M$ if $p \gg 2\pi/R_{TF}$. Consequently for a given detuning ν, molecules with momenta in a shell of radius $2\sqrt{M\nu}$ and width $2\pi/R_{\mathrm{TF}}$ are formed from one atom in the condensate and another atom taken from the noncondensed part with a momentum that lies in a sphere in momentum space around $\mathbf{p}$ with radius $2\pi/R_{\mathrm{TF}}$. Momentum and energy conservation are illustrated in Fig. 2. Figure 3 shows a typical example for the momentum distribution.

Equation (20) allows us to extract the criterion for the applicability of our approximation scheme, i.e., of treating the atomic state as being undepleted. The coherent contribution will only be nonzero if $|\mathbf{p}| \leqslant 2\pi/R_{TF}$ and for these momenta the incoherent contribution can be neglected, as we have seen. Requiring that the number of molecules remains much smaller then the initial number of atoms leads to the condition

$$\sqrt{N}g \ll \nu \frac{1}{R_{TF}^3 (M\nu)^{3/2}}. \tag{22}$$

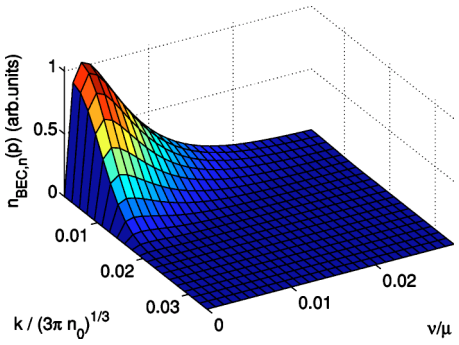

FIG. 3. (Color online) Momentum distribution of molecules formed from a BEC of $N=10^5$ atoms with scattering length $a = 0.01a_{\mathrm{osc}}$ at $T = 0.1T_c$ for a narrow resonance.

In the opposite case $|\mathbf{p}| > 2\pi/R_{TF}$ the coherent contribution is essentially zero and we need only consider the incoherent contribution. Requiring that the number of molecules with momentum $\mathbf{p}$ be much smaller than the number of noncondensed atoms with that same momentum leads to

$$gt \ll N^{-1}\frac{\nu}{g}\frac{1}{R_{TF}^3 (M\nu)^{3/2}}. \tag{23}$$

IV. NORMAL FERMI GAS

For a normal Fermi gas (NFG) we restrict ourselves to the case of zero temperature, $T=0$. For temperatures T well below the Fermi temperature T_F, the corrections to our results are of order $(T/T_F)^2$ or higher, and do not lead to any qualitatively new effects.

Again, we treat the gas in the local density approximation where the atoms locally fill a Fermi sea

$$|\mathrm{NFG}\rangle = \prod_{|\mathbf{k}|<k_F(\mathbf{x})} \hat{c}_{\mathbf{k}}^{\dagger}|0\rangle \tag{24}$$

with local Fermi momentum $k_F(\mathbf{x})$ and $|0\rangle$ being the atomic vacuum. The Fermi momentum is related to the local chemical potential

$$\mu_{\mathrm{loc}}(\mathbf{x}) = \mu_0 - U_{\mathrm{tr}}(\mathbf{x}) \tag{25}$$

by means of

$$\mu_{\mathrm{loc}}(\mathbf{x}) = \frac{k_F^2(\mathbf{x})}{2M} = \frac{[3\pi^2 n(\mathbf{x})]^{2/3}}{2M}. \tag{26}$$

Here, $\mu_0 = (3\pi^2 n_0)^{2/3}/(2M)$ is the chemical potential of the trapped gas, and n_0 is the density at the center of the trap for each of the spin states. The Hartree-Fock mean field has been neglected because it gives rise only to minor corrections and does not lead to a qualitatively new behavior. The density distribution of the trapped gas is given by the Thomas-Fermi result [40],

$$n(\mathbf{x}) = \frac{N}{R_F^3}\frac{8}{\pi^2}\left[1 - \frac{r^2}{R_F^2}\right]^{3/2}, \tag{27}$$

where $R_F = (48N)^{1/6}a_{\mathrm{osc}}$ is the Thomas-Fermi radius for fermions.

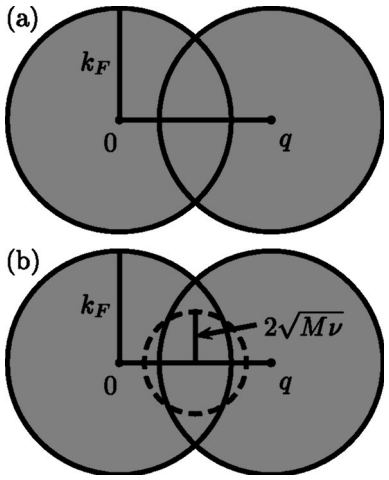

FIG. 4. (a) Illustration of the number of atom pairs with center of mass momentum q. Atoms in the intersection of the two shifted Fermi spheres can be transformed into a molecule of momentum q if energy conservation plays no role. (b) Density of atom pairs with center of mass momentum q and total kinetic energy $2\sqrt{M\nu}$. In addition to lying in the intersection of the two Fermi spheres the atoms also have to lie on a shell of radius $2\sqrt{M\nu}$ in order to satisfy energy conservation.

Using the same perturbation methods as described in the previous section for bosons, we can calculate the momentum distribution of the molecules and their correlation function $g^{(2)}$ for a broad and for a narrow resonance by first calculating the density of the desired quantity at a position $\mathbf{x}$ and then integrating the result over the volume of the gas.

A. Broad resonance $E_{\mathrm{kin}} \ll g\sqrt{N}$

To deal with the case of fermions, we modify Eq. (6) by reintroducing the spin of the atoms. The integral over the relative momentum of the atom pairs can be carried out exactly to give

$$n_{\mathrm{NFG},b}(\mathbf{p},\mathbf{x},t) = \begin{cases} (gt)^2 F_b(\mathbf{p},\mathbf{x}), & |\mathbf{p}| \leqslant 2k_F(\mathbf{x}) \\ 0, & |\mathbf{p}| > 2k_F(\mathbf{x}), \end{cases} \tag{28}$$

where we have introduced the local density of atom pairs with center of mass momentum $\mathbf{p}$,

$$F_b(\mathbf{p},\mathbf{x}) = \frac{\pi k_F^3(\mathbf{x})}{12}\left[16 - 12\frac{|\mathbf{p}|}{k_F(\mathbf{x})} + \left(\frac{|\mathbf{p}|}{k_F(\mathbf{x})}\right)^3\right]. \tag{29}$$

$F_b(\mathbf{p},\mathbf{x})$ can be visualized as the integral over the intersection of two Fermi seas shifted by $\mathbf{p}$ relative to each other, as depicted in Fig. 4(a).

The characteristic width of the momentum distribution of the molecules is $k_F \propto n_0^{1/3}$ which is typically much wider than the distribution found in the BEC case. From Eq. (28) the number of molecules produced scales linearly with the number of atoms. This is because in contrast to the BEC case, the molecule production is a noncollective effect. Each atom pair is converted into a molecule independently of all the others and there is no collective enhancement. The integration of these results over the volume of the cloud can easily be done numerically and is shown in the inset in Fig. 1.

Similarly, we can calculate the local value of $g^{(2)}$ at position $\mathbf{x}$, from Eq. (14),

$$\begin{aligned} g^{(2)}_{\mathrm{loc}}(\mathbf{p_1},t_1;\mathbf{p_2},t_2) = \Bigg\{ & F_b(\mathbf{p_1},\mathbf{x})F_b(\mathbf{p_2},\mathbf{x}) - \int d\mathbf{k} n(\mathbf{p_2}/2 \\ & + \mathbf{k}) n(\mathbf{p_2}/2 - \mathbf{k}) n(\mathbf{p_1} - \mathbf{p_2}/2 - k) \\ & - \int d\mathbf{k} n(\mathbf{p_2} + \mathbf{k} - \mathbf{p_1}/2) n(\mathbf{p_1}/2 + \mathbf{k}) n(\mathbf{p_1}/2 \\ & - \mathbf{k}) + \int d\mathbf{k} n(\mathbf{p_2} - \mathbf{p_1}/2 + \mathbf{k}) n(\mathbf{p_1}/2 \\ & - \mathbf{k_1}) n(\mathbf{p_2}/2 - \mathbf{k_2}) \Bigg\} \Bigg/ F_b(\mathbf{p_1},\mathbf{x})F_b(\mathbf{p_2},\mathbf{x}). \end{aligned} \tag{30}$$

This result simplifies considerably for $\mathbf{p}_1 = \mathbf{p}_2 = \mathbf{p}$,

$$g^{(2)}_{\mathrm{loc}}(\mathbf{p},\mathbf{x},t) \equiv g^{(2)}_{\mathrm{loc}}(\mathbf{p},t;\mathbf{p},t,\mathbf{x}) = 2\left(1 - \frac{1}{F_b(\mathbf{p},\mathbf{x})}\right). \tag{31}$$

As in the case of the BEC, the time dependence in $g^{(2)}(\mathbf{p},\mathbf{x},t)$ cancels at this level of approximation. However, in contrast to the case of a BEC there is some dependence on the momentum left.

The origin of the factor of two in $g^{(2)}(\mathbf{p},\mathbf{x},t)$ is the following: The two molecules that are being detected in the measurement of $g^{(2)}$ can be formed from four atoms in two different ways and the two possibilities both give the same contribution. Equation (31) indicates that the statistics of the molecules are super-Poissonian, similarly to a thermal field.

By the following argument we can convince ourselves that not only the second-order correlations look thermal, but that the entire counting statistics of each momentum mode is thermal. Each molecular mode characterized by the momentum $\mathbf{p}$ is coupled to a particular subset of atom pairs selected by momentum conservation. In the short-time limit, each atom pair with center-of-mass momentum $\mathbf{p}$ is converted into a molecule in the corresponding molecular mode independently of all the other atom pairs and with uncorrelated phases. Thus we expect the number statistics of each molecular mode to be similar to that of a light field in thermal equilibrium with a reservoir with which there is an incoherent exchange of energy.

B. Narrow resonance, $E_{kin} \gg g\sqrt{N}$

In this case, the molecules formed have to satisfy energy and momentum conservation, as illustrated in Fig. 4(b). We are then led to a calculation very similar to the one presented in Appendix B for the contribution from the noncondensed fraction of atoms for the BEC case. After integrating over the volume of the cloud we find

$$n_{\mathrm{NFG},n}(\mathbf{p},t) = \frac{g^2 t}{8\pi} M^{3/2} \nu^{1/2} \times \int d^3x \, \max\left[0, \min\left(2, \frac{k_F(\mathbf{x})^2 - p^2/4 - M\nu}{|\mathbf{p}|\sqrt{M\nu}}\right)\right]. \tag{32}$$

The number of molecules produced is proportional to the number of atom pairs that satisfy momentum and energy conservation and hence scales linearly with the number of atoms, indicating that molecule formation is not a collective effect. Figure 5 shows the momentum distribution for typical parameters. It is much wider than the momentum distribution for the BEC case in both momentum space and in energy width.

We do not give the lengthy and complicated expression for $g^{(2)}_{\mathrm{loc}}(\mathbf{p}_1,t_1,\mathbf{p}_2,t_2)$ because its qualitative properties are the same as those in the broad resonance case except that the integration is now over pairs of atoms that also satisfy energy conservation. For the particular case of $\mathbf{p}_1=\mathbf{p}_2=\mathbf{p}$, we obtain an expression with the exact same form as Eq. (31) except that $F_b(\mathbf{p},\mathbf{x})$ must be replaced with $F_n(\mathbf{p},\nu,\mathbf{x})$,

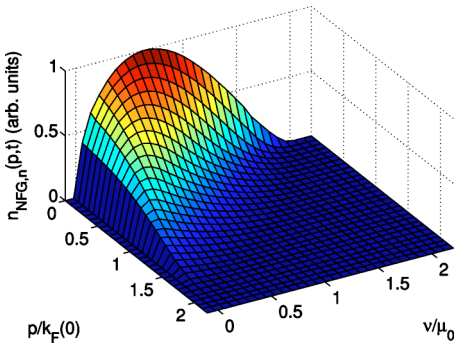

FIG. 5. (Color online) Momentum distribution of molecules produced from a normal Fermi gas in the narrow resonance limit for $g=10^{-3}\,\mu$.

$$F_n(\mathbf{p},\nu,\mathbf{x}) = \begin{cases} \dfrac{M^{3/2}}{4\pi^2}\sqrt{\nu}, & \sqrt{M\nu} \leqslant k_F(\mathbf{x}) - p/2 \\ \dfrac{k_F(\mathbf{x})^2 - p^2/4 - M\nu}{|\mathbf{p}|\sqrt{M\nu}}, & k_F(\mathbf{x}) - p/2 \leqslant \sqrt{M\nu} \leqslant k_F(\mathbf{x}) + p/2 \\ 0, & \sqrt{M\nu} \geqslant k_F(\mathbf{x}) + p/2 \end{cases} \tag{33}$$

which depends on $\mathbf{p}$ only in the intermediate region of detunings $k_F(\mathbf{x}) - p/2 \leqslant \sqrt{M\delta} \leqslant k_F(\mathbf{x}) + p/2$.

V. BCS STATE

Let us now consider a system of fermions with attractive interactions, $U_0 < 0$, at temperatures well below the BCS critical temperature. As is well known, for these temperatures the attractive interactions give rise to correlations between pairs of atoms in time-reversed states known as Cooper pairs. We assume that the spherically symmetric trapping potential is sufficiently slowly varying that the gas can be treated in the local-density approximation. More quantitatively, the local-density approximation is valid if the size of the Cooper pairs, given by the correlation length

$$\lambda(r) = v_F(r)/\pi\Delta(r),$$

is much smaller than the oscillator length for the trap. Here, $v_F(r)$ is the velocity of atoms at the Fermi surface and $\Delta(r)$ is the pairing field at distance r from the origin, which we take at the center of the trap.

Before turning to the coupled atom-molecule system we outline our treatment of the atomic system. We closely follow the approach of Houbiers *et al.* [41]. We assume that locally at each r, the wave function can be approximated by the BCS wave function for a homogenous gas,

$$|\mathrm{BCS}(r)\rangle = \prod_{\mathbf{k}} [u_{\mathbf{k}}(r) + v_{\mathbf{k}}(r)\hat{c}^\dagger_{-\mathbf{k},\uparrow}\hat{c}^\dagger_{\mathbf{k},\downarrow}]|0\rangle, \tag{34}$$

with Bogoliubov amplitudes

$$u^2_{\mathbf{k}}(r) = \frac{1}{2}\left(1 + \frac{\xi_{\mathbf{k}}(r)}{\sqrt{\Delta^2(r) + \xi^2_{\mathbf{k}}(r)}}\right), \tag{35}$$

$$v^2_{\mathbf{k}}(r) = \frac{1}{2}\left(1 - \frac{\xi_{\mathbf{k}}(r)}{\sqrt{\Delta^2(r) + \xi^2_{\mathbf{k}}(r)}}\right). \tag{36}$$

Here $\xi_{\mathbf{k}}(r) = \epsilon_{\mathbf{k}} - \mu_{\mathrm{loc}}(r)$ is the kinetic energy of an atom measured from the local chemical potential defined as

$$\mu_{loc}(r) = \mu_0 - U(r) - U_0 n(r). \tag{37}$$

In contrast to the normal Fermi gas, we have included a Hartree-Fock mean-field energy to the local chemical potential since we can no longer ignore the effect of the two-body interactions in the gas. To an excellent approximation we can use the relation Eq. (26) between density and local chemical potential. Then, for a given number of atoms N, Eq. (37) is an implicit equation for μ_0. We solve it numerically and hence determine the density profile $n(r)$ and the local chemical potential $\mu_{\mathrm{loc}}(r)$.

The gap parameter $\Delta(r)=U_0/2V\Sigma_k u_{\mathbf{k}}(r)v_{\mathbf{k}}(r)$ is determined by the gap equation

$$\frac{-\pi}{2k_F(0)a}=\mu_0 k_F^{-3}(0)\int_0^\infty dk k^2\left(\frac{1}{\sqrt{\xi_{\mathbf{k}}^2(r)+\Delta^2(r)}}-\frac{1}{\xi_{\mathbf{k}}(r)}\right), \tag{38}$$

where the ultraviolet divergence has been removed by renormalizing the bare background scattering strength to the two-body T-matrix using the Lippmann-Schwinger equation (see Ref. [41]). We solve the gap equation numerically using the previously determined local chemical μ_{loc}.

A. Broad resonance, $E_{kin}\ll g\sqrt{N}$

We find the momentum distribution of the molecules from the BCS-type state by repeating the calculation done in the case of a normal Fermi gas. For the BCS wave function, the relevant atomic expectation values factorize as

$$\begin{aligned}\langle \hat{c}^\dagger_{\mathbf{p}/2-\mathbf{k_1},\uparrow}\hat{c}^\dagger_{\mathbf{p}/2+\mathbf{k_1},\downarrow}\hat{c}_{\mathbf{p}/2+\mathbf{k_2},\uparrow}\hat{c}_{\mathbf{p}/2-\mathbf{k_2},\downarrow}\rangle &= \langle \hat{c}^\dagger_{\mathbf{p}/2-\mathbf{k_1},\uparrow}\hat{c}^\dagger_{\mathbf{p}/2+\mathbf{k_1},\downarrow}\rangle\langle \hat{c}_{\mathbf{p}/2+\mathbf{k_2},\downarrow}\hat{c}_{\mathbf{p}/2-\mathbf{k_2},\uparrow}\rangle \\ &+\langle \hat{c}^\dagger_{\mathbf{p}/2-\mathbf{k_1},\uparrow}\hat{c}_{\mathbf{p}/2+\mathbf{k_2},\downarrow}\rangle\langle \hat{c}^\dagger_{\mathbf{p}/2+\mathbf{k_1},\downarrow}\hat{c}_{\mathbf{p}/2-\mathbf{k_2},\uparrow}\rangle\end{aligned} \tag{39}$$

and the momentum distribution of the molecules becomes

$$\begin{aligned}n_{\mathrm{BCS},b}(\mathbf{p},t) &= (gt)^2\left[\left|\sum_k \langle \hat{c}_{\mathbf{p}/2+\mathbf{k},\downarrow}\hat{c}_{\mathbf{p}/2-\mathbf{k},\uparrow}\rangle\right|^2 + \sum_{\mathbf{k}}\langle \hat{c}^\dagger_{\mathbf{p}/2-\mathbf{k},\uparrow}\hat{c}_{\mathbf{p}/2+\mathbf{k},\downarrow}\rangle\langle \hat{c}^\dagger_{\mathbf{p}/2+\mathbf{k},\downarrow}\hat{c}_{\mathbf{p}/2-\mathbf{k},\uparrow}\rangle\right] \\ &\approx (gt)^2\left|\sum_k \langle \hat{c}_{\mathbf{p}/2+\mathbf{k},\downarrow}\hat{c}_{\mathbf{p}/2-\mathbf{k},\uparrow}\rangle\right|^2 + n_{\mathrm{NFG},b}(\mathbf{p},t).\end{aligned} \tag{40}$$

In going from the first to the second line we have assumed that the interactions are weak enough so that the momentum distribution of the atoms is essentially that of a two-component Fermi gas. This is justified because the Cooper pairing only affects the momentum distribution in a small shell of thickness $1/\lambda(r)\ll k_F(r)$ around the Fermi surface.

The first term involves the square of the pairing field. It is proportional to the square of the number of paired atoms which, below the critical temperature, is a finite fraction of the total number of atoms. This quadratic dependence indicates that it is the result of a collective effect. This term can be related to the two-point correlation function in position space as

$$\langle \hat{c}_{\mathbf{p}/2+\mathbf{k},\downarrow}\hat{c}_{\mathbf{p}/2-\mathbf{k},\uparrow}\rangle = \int \frac{d^3x d^3r}{V} e^{-i\mathbf{p}\cdot\mathbf{x}-i\mathbf{k}\cdot\mathbf{r}}\langle \hat{\psi}_\downarrow(\mathbf{x}-\mathbf{r}/2)\hat{\psi}_\uparrow(\mathbf{x}+\mathbf{r}/2)\rangle, \tag{41}$$

where $\hat{\psi}_{\uparrow,\downarrow}$ are the atomic field operators in position space. In the local-density approximation, the correlation function varies with $\mathbf{x}$ on a length scale R_{TF}. On the other hand, the expectation value in the integral falls off to zero for $r>\lambda(r)$ and we can therefore treat the correlation function as being independent of $\mathbf{x}$ when performing the integration over $\mathbf{r}$,

$$\langle \hat{c}_{\mathbf{p}/2+\mathbf{k},\downarrow}\hat{c}_{\mathbf{p}/2-\mathbf{k},\uparrow}\rangle = \int \frac{d^3x}{V} e^{-i\mathbf{p}\cdot\mathbf{x}}\langle \hat{c}_{\mathbf{k},\downarrow}\hat{c}_{-\mathbf{k}\uparrow}\rangle_x. \tag{42}$$

The expectation value on the right-hand side is evaluated using the local-density approximation at position x. Inserting the result into Eq. (40) and making use of the gap equation we find

$$n_{\mathrm{BCS},b}(\mathbf{p},t) = (gt)^2\left[\left|\int d^3x e^{-i\mathbf{x}\cdot\mathbf{p}}\left(1-\frac{2a\Lambda}{\pi}\right)\frac{2\Delta(x)}{U_0}\right|^2 + n_{\mathrm{NFG},b}(\mathbf{p},t)\right]. \tag{43}$$

Following Ref. [41] we have replaced the bare background coupling strength by

$$U_0 = U_0\frac{1}{1-\dfrac{2a\Lambda}{\pi}}, \tag{44}$$

where Λ is a momentum cutoff and is of the order of the inverse of the range of the interatomic potential.

Using the numerically determined $\Delta(x)$ we can readily perform the remaining Fourier transform in Eq. (43). The result of such a calculation is shown in Fig. 1. Since the gap parameter changes over distances of order R_{TF} the contribution from the pairing field has a typical width of order $1/R_{TF}$. This is very similar to the BEC case. The background from the unpaired atoms on the other hand has a typical width $k_F(0)=(3\pi^2 n_0)^{1/3}$ which is similar to the width of the noise contribution in the BEC case, see the inset in Fig. 1. This similarity can be understood by recalling that for a weakly interacting condensate, $n_0^{1/3}a=\beta\ll 1$, which when substituted into the definition of the healing length gives $1/\xi=(8\pi\beta)^{1/2}n_0^{1/3}$. For typical $\beta\sim 0.1$, this is comparable to $k_F(0)$ for equal densities.

Because of the collective nature of the coherent contribution it will dominate over the background $n_{\mathrm{NFG},b}$ for strong enough interactions and large enough particle numbers. The narrow width and the collective enhancement of the molecule production are the reasons why the momentum distribution of the molecules is such an excellent indicator of the presence of a superfluid component and the off-diagonal long-range order accompanying it.

For weak interactions such that the coherent contribution is small compared to the incoherent contribution, the second-order correlations are close to those of a normal Fermi gas given by Eq. (31), $g^{(2)}(\mathbf{p},\mathbf{x},t)\approx 2$. However, in the strongly interacting regime, $k_F|a|\sim 1$, and large N, the coherent contribution from the paired atoms dominates over the incoherent contribution from unpaired atoms. In this limit one finds that the second-order correlation is close to that of the BEC, $g^{(2)}(\mathbf{p},\mathbf{x},t)\approx 1$. The physical reason for this is that at the level of even-order correlations the pairing field behaves just like the mean field of the condensate. This is clear from the factorization property of the atomic correlation functions,

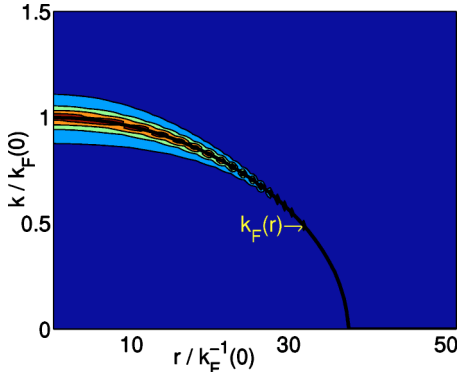

FIG. 6. (Color online) Pairing field $\langle \hat{c}_{\mathbf{k},\downarrow}\hat{c}_{-\mathbf{k},\uparrow}\rangle = u_k v_k$ across the trap for $k_F a = 0.5$ and $a_{\mathrm{osc}} = 5k_F^{-1}(0)$. The black solid line indicates the local Fermi momentum $k_F(r)$.

Eq. (39), in terms of the normal component of the density and the anomalous density contribution due to the mean field. In this case, the leading-order terms in N are given by the anomalous averages. In the strongly interacting limit, the contribution from the "unpaired" atoms is very similar in nature to the contribution from the fluctuations in the BEC case.

B. Narrow resonance, $E_{\mathrm{kin}} \gg g\sqrt{N}$

A calculation similar to the one presented in Appendix B for the BEC case leads to

$$n_{\mathrm{BCS},n}(\mathbf{p},t) = \left| \sum_{\mathbf{k}} \Delta(\nu - k^2/M)\langle \hat{c}_{\mathbf{p}/2+\mathbf{k},\downarrow}\hat{c}_{\mathbf{p}/2-\mathbf{k},\uparrow}\rangle \right|^2 + n_{\mathrm{NFG},n}(\mathbf{p},t), \tag{45}$$

where we have assumed again that the gas is weakly interacting. Inserting Eq. (19) for Δ in the limit $\nu t \to \infty$ and performing similar manipulations as in the broad resonance case leads to

$$n_{\mathrm{BCS},n}(\mathbf{p},t) = \frac{g^2 M^3}{\pi^2 p^2} \left| \int_0^\infty d\omega \sqrt{\omega} \left(\pi\delta(\nu-\omega) + i\mathbf{P}\frac{1}{\nu-\omega} \right) \times \int_0^{R_{\mathrm{TF}}} dr\, r \sin(pr)\, \langle \hat{c}_{\sqrt{M\omega},\downarrow}\hat{c}_{-\sqrt{M\omega},\uparrow}\rangle|_r \right|^2 + n_{\mathrm{NFG},n}, \tag{46}$$

where again the pairing field $\langle \hat{c}_{k,\downarrow}\hat{c}_{-k,\uparrow}\rangle|_r = u_k(r)v_k(r)$ can be evaluated using the local-density approximation. Figure 6 shows an example of the pairing field across the trap. Two qualitatively different cases have to be distinguished depending on the strength of the interactions.

If the interactions are fairly strong so that the pairing field, $u_k(r)v_k(r)$, is nonzero in a rather wide region around $k_F(r)$, the pairing field will be a slowly varying function across the atomic cloud. Then the remaining integral in Eq. (46) can be easily evaluated numerically and we find a momentum distribution of the molecules which is similar to the BEC case. This limit is illustrated in Fig. 7. The width of the momentum distribution of the molecules is again of order

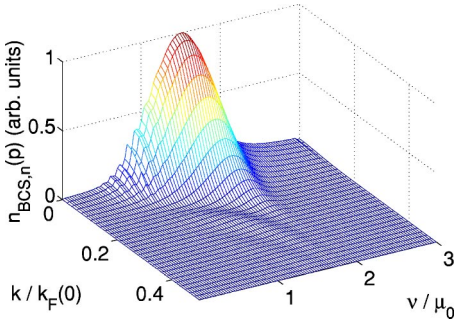

FIG. 7. (Color online) Momentum distribution of molecules formed from a strong coupling ($k_F a = 0.5$) BCS system in the narrow resonance regime as a function of detuning ν for $a_{\mathrm{osc}} = 5k_F^{-1}(0)$. Well below $\nu = 2\mu$ the figure is a bit noisy because the Fourier transform in Eq. (46) gets its main contribution from a very narrow region in space where the solution of the gap equation is numerically challenging.

$1/R_{TF}$. It is known that in the strongly interacting limit, the size of the Cooper pairs becomes comparable to the interparticle spacing, $\lambda(r) \sim 1/k_F(r)$. The Cooper pairs are no longer delocalized across the extent of the cloud but now approach the limit of localized Bosonic "quasimolecules." Thus it is not surprising that the momentum distribution of molecules formed from a BCS-type state approaches the one we found in the BEC case.

On the other hand, if the interactions between the atoms are weak the pairing field is a very narrow function of momentum and hence, for fixed momentum, also of position as can be seen from Fig. 6. Then the integral in Eq. (46) has contributions from a rather narrow region in space only and the momentum distribution will accordingly become wider and smaller.

Probing the BCS system in the narrow resonance regime also yields spatial information about the atomic state. By tuning $\nu = 2\mu_{\mathrm{loc}}(r)$ the molecular signal is most sensitive to the pairing field near r and less sensitive to other regions in the trap.

A qualitative difference between the BCS and BEC cases becomes apparent if one looks at the number of molecules as a function of the detuning. While we find that there is only a very narrow distribution of detunings with width $\sim(2\pi/R_{TF})^2/2M$ that leads to molecule formation in the BEC case, molecules are being formed for detunings well below $\nu \sim 2\mu_0$. The nonhomogeneity of the trapped atom system manifests itself in a completely different way in the two cases. In the BEC case, the total energy of a particle in the condensate is just the chemical potential while the kinetic energy of a particle is very small compared to the mean-field energy in the Thomas Fermi limit. Upon release, the atoms in the condensate all have a spread in kinetic energies that is of the order $(2\pi/R_{TF})^2/2M$ due entirely to zero-point motion. On the other hand, in the BCS case the superfluid forms at each position near the local Fermi momentum. Hence atoms in the BCS state have a large energy spread that is of the order $\sim\mu_0$ with the kinetic energies of the paired atoms being centered around $\mu_{\mathrm{loc}}(r)$ with a width $\Delta(r)$.

For the second-order moment, $g^{(2)}(\mathbf{p},\mathbf{x},t)$, the same general arguments that were put forward in the discussion of the

broad resonance also apply to the narrow resonance. In the strongly interacting limit, the molecular field is again approximately coherent with a noise contribution from the unpaired fermions.

VI. SUMMARY

We examined the momentum distribution and momentum correlations of molecules formed by a Feshbach resonance or by photoassociation from a quantum degenerate atomic gas. Our study elucidated the effect of the atomic trapping potential as well as the strength of the atom-molecule coupling relative to the characteristic energies of the atoms on the molecular momentum distribution.

Molecules produced from an atomic BEC show a rather narrow momentum distribution that is comparable to the zero-point momentum width of the atomic BEC from which they are formed. In the case of a narrow resonance, energy conservation limits the molecules to only a narrow energy range. The molecule production is a collective effect with contributions from all atom pairs adding up constructively, as indicated by the quadratic scaling of the number of molecules with the number of atoms. Each mode of the resulting molecular field is to a very good approximation coherent [up to terms of order $\mathcal{O}(1/N)$]. The effects of noise, both due to finite temperatures and to vacuum fluctuations, are of relative order $\mathcal{O}(1/N)$. They slightly increase the $g^{(2)}$ and cause the molecular field in each momentum state to be only partially coherent.

In contrast, the momentum distribution of molecules formed from a normal Fermi gas is much broader with a typical width given by the Fermi momentum of the initial atomic cloud. The molecule production is not collective as the number of molecules only scales like the number of atoms rather than the square. In this case, the second-order correlations of the molecules exhibit super-Poissonian fluctuations, and it was argued that the molecules are well characterized by a thermal field.

The case where molecules are produced from paired atoms in a BCS-like state shares many properties with the BEC case: The molecule formation rate is collective, their momentum distribution is very narrow in comparison to the normal Fermi gas, and the molecular field is essentially coherent. The noncollective contribution from unpaired atoms has a momentum distribution very similar to that of the quasiparticle fluctuations in the BEC case.

In a future publication we will use the Bogoliubov–de Gennes equations to describe the BCS-type state which is again probed with a molecular field. Thus we will be able to go beyond the local-density approximation and we can study the BEC-BCS crossover regime. Also, this will allow us to study the validity of the local-density approximation more carefully.

ACKNOWLEDGMENTS

This work was supported in part by the US Office of Naval Research, by the National Science Foundation, by the US Army Research Office, and by the National Aeronautics and Space Administration.

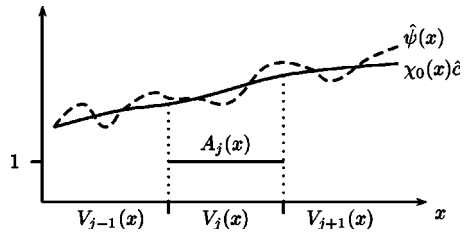

FIG. 8. Illustration of the partitioning of quantization volume and atomic field operator. Also indicated is the function $A_j(\mathbf{x})$.

APPENDIX A: CALCULATION OF $n(\mathbf{p})$ FOR $g \gg E_{kin}$ FOR A BEC

In this appendix we show how the decomposition of the atomic field operator into condensed and noncondensed fraction together with the local-density approximation for the noncondensed part can be used to calculate the momentum distribution of the molecules for the case of an initial BEC of atoms. More details on the properties of fluctuations at nonzero temperatures and the use of the local-density approximation for their description can be found in Refs. [37–39].

The starting point of our calculation is Eq. (6) for the momentum distribution of the molecules. It reduces the problem to evaluating an integral over expectation values in the undisturbed atomic field at $t=0$. The relevant expectation values are most transparently calculated by partitioning the quantization volume V into smaller volumes V_j that are larger than the coherence length ξ. Partitioning the atomic field operator accordingly, we get

$$\hat{\psi}(\mathbf{x}) = \sum_j A_j(\mathbf{x})\chi_0(\mathbf{x})\hat{c} + \sum_j \delta\hat{\psi}^{(j)}_{\mathrm{loc}}(\mathbf{x}), \tag{A1}$$

where we have introduced functions $A_j(\mathbf{x})$ that are one in volume V_j and zero otherwise, and $\delta\hat{\psi}^{(j)}_{\mathrm{loc}}(x)=A_j(x)\delta\hat{\psi}(x)$. The partitioning of the field operator is illustrated in Fig. 8. We go over to the Fourier transform

$$\hat{c}_{\mathbf{p}} = \int \frac{d^3x}{\sqrt{V}} e^{-i\mathbf{p}\cdot\mathbf{x}}\hat{\psi}(\mathbf{x}) = \tilde{\chi}_0(\mathbf{p})\hat{c} + \sum_{V_j} \sqrt{\frac{V_j}{V}}\delta\hat{c}^{(j)}_{\mathbf{p}}, \tag{A2}$$

where $\delta\hat{c}^{(j)}(\mathbf{p})$ is the annihilation operator for a fluctuation of momentum $\mathbf{p}$ in volume V_j. In the local-density approximation, fluctuations in different cells V_j are uncorrelated and we have

$$\langle \delta\hat{c}^{(i)\dagger}_{\mathbf{k}_1}\delta\hat{c}^{(j)}_{\mathbf{k}_2}\rangle \equiv \delta_{i,j}\delta_{\mathbf{k}_1,\mathbf{k}_2}\langle \delta\hat{c}^{(i)\dagger}_{\mathbf{k}_1}\delta\hat{c}^{(i)}_{\mathbf{k}_1}\rangle. \tag{A3}$$

Inserting in Eq. (6), keeping only terms of first order in the fluctuations and making use of relation (A3) we find

$$\begin{aligned} n_{\mathrm{BEC},b}(\mathbf{p},t) = (gt)^2 N(N-1)\sum_{\mathbf{k}_1,\mathbf{k}_2} &\tilde{\chi}_0^*(\mathbf{p}/2-\mathbf{k}_1)\tilde{\chi}_0^*(\mathbf{p}/2 \\ &+\mathbf{k}_1)\tilde{\chi}_0(\mathbf{p}/2-\mathbf{k}_2)\tilde{\chi}_0(\mathbf{p}/2+\mathbf{k}_2) \\ &+ 4(gt)^2 N\sum_{\mathbf{k},j}\frac{V_j}{V}|\tilde{\chi}_0(\mathbf{p}-\mathbf{k})|^2\langle \hat{c}^{(j)\dagger}_{\mathbf{k}}\hat{c}^{(j)}_{\mathbf{k}}\rangle. \end{aligned} \tag{A4}$$

The coherent term is readily brought to the form given in Eq. (7). In the incoherent term we notice that $|\tilde{\chi}_0(\mathbf{p})|^2$ is a much narrower function than $\langle \hat{c}_{\mathbf{k}}^{(j)\dagger}\hat{c}_{\mathbf{k}}^{(j)}\rangle$, the former having a typical width of $\sim 1/R_{TF}$ while the latter has a typical width of $\sim 1/\xi$. Hence, to a good approximation, $\langle \hat{c}_{\mathbf{k}}^{(j)\dagger}\hat{c}_{\mathbf{k}}^{(j)}\rangle$ can be treated as a constant for the momentum range for which $|\tilde{\chi}_0(\mathbf{p})|^2$ is nonzero and we obtain

$$\begin{aligned} &4(gt)^2 N \sum_{\mathrm{k},j} \frac{V_j}{V} |\tilde{\chi}_0(\mathbf{p}-\mathbf{k})|^2 \langle \hat{c}_{\mathbf{k}}^{(j)\dagger}\hat{c}_{\mathbf{k}}^{(j)}\rangle \\ &\approx 4(gt)^2 N \sum_j \frac{V_j}{V} \langle \hat{c}_{\mathbf{k}}^{(j)\dagger}\hat{c}_{\mathbf{k}}^{(j)}\rangle \sum_{\mathbf{k}} |\tilde{\chi}_0(\mathbf{p}-\mathbf{k})|^2 \\ &= 4(gt)^2 N \sum_j \frac{V_j}{V} \langle \hat{c}_{\mathbf{k}}^{(j)\dagger}\hat{c}_{\mathbf{k}}^{(j)}\rangle, \end{aligned} \tag{A5}$$

where we have made use of the normalization of $\chi_0(\mathbf{x})$ in the last step. Since $\xi \ll R_{TF}$ the volumes V_j can be made small and the sum can be approximated by an integral, leading to Eq. (7).

APPENDIX B: CALCULATION OF $n(\mathbf{p})$ FOR $g \ll E_{kin}$ FOR A BEC

The calculation goes along similar lines as in the broad resonance case but the evaluation of the integrals is more complicated. Repeating the calculation of the broad resonance case that led to Eq. (A4) with $\hat{a}_{\mathbf{p}}$ now replaced according to Eq. (18) we find, again to first order in the fluctuations,

$$\begin{aligned} n_{\mathrm{BEC},n}(\mathbf{p},t) &= N(N-1)\Bigg| \sum_{\mathbf{k}} \Delta(E_{\mathbf{p}} - \epsilon_{\mathbf{p}/2+\mathbf{k}} - \epsilon_{\mathbf{p}/2-\mathbf{k}}, t)\tilde{\chi}_0(\mathbf{p}/2 \\ &\quad + \mathbf{k})\tilde{\chi}_0(\mathbf{p}/2-\mathbf{k})\Bigg|^2 + 4N\sum_{\mathbf{k},j} \frac{V^j}{V} |\Delta(E_{\mathbf{p}} - \epsilon_{\mathbf{p}/2+\mathbf{k}} \\ &\quad - \epsilon_{\mathbf{p}/2-\mathbf{k}}, t)|^2 |\tilde{\chi}_0(\mathbf{p}-\mathbf{k})|^2 \langle \hat{c}_{\mathbf{k}}^{(j)\dagger}\hat{c}_{\mathbf{k}}^{(j)}\rangle \\ &\equiv n_{\mathrm{coh}}(\mathbf{p},t) + n_{\mathrm{incoh}}(\mathbf{p},t). \end{aligned} \tag{B1}$$

Let us first consider the coherent part $n_{\mathrm{coh}}(\mathbf{p},t)$. Going over from the summation to an integral in the usual way, making the substitution $\omega = k^2/M$ and introducing polar coordinates we find

$$\begin{aligned} n_{\mathrm{coh}}(\mathbf{p},t) &= \frac{VM^{3/2}}{\pi^2 2^3} \int_0^\infty d\omega \Delta(\nu-\omega,t) \int_0^\pi d\vartheta \sin\vartheta \sqrt{\omega}\tilde{\chi}_0 \\ &\quad \times \left(\sqrt{p^2/4 + M\omega + |p|\sqrt{M\omega}\cos\vartheta}\right)\tilde{\chi}_0 \\ &\quad \times \left(\sqrt{p^2/4 + M\omega - |p|\sqrt{M\omega}\cos\vartheta}\right). \end{aligned} \tag{B2}$$

In the limit $t\to\infty$, $\Delta(\nu-\omega)$ becomes [42]

$$\lim_{t\to\infty} \Delta(\nu-\omega,t) = g\left(\pi\delta(\nu-\omega) - i\mathbf{P}\frac{1}{\nu-\omega}\right), \tag{B3}$$

where, as usual, **P** means that the integral has to be taken in the sense of the Cauchy-principal value. The real part can be evaluated by making use of the δ function and for the imaginary part we have to rely on numerical methods to calculate the principal value integral.

Making similar manipulations of the sums over momenta for the incoherent part leads to

$$\begin{aligned} n_{\mathrm{incoh}}(\mathbf{p},t) &= 4N\frac{M^{3/2}}{8\pi^2}\sum_j V_j \int_0^\pi d\vartheta \sin\vartheta \\ &\quad \times \int_0^\infty d\omega\sqrt{\omega}|\Delta(\nu-\omega,t)|^2 |\tilde{\chi}_0 \\ &\quad \times \left(\sqrt{p^2/4 + M\omega - |p|\sqrt{M\omega}\cos\vartheta}\right)|^2 \langle \hat{c}_{\sqrt{M\omega}}^{(j)\dagger}\hat{c}_{\sqrt{M\omega}}^{(j)}\rangle. \end{aligned} \tag{B4}$$

Using the delta function

$$\lim_{t\to\infty} |\Delta(\nu-\omega)|^2 = \pi g^2 t \delta(\nu-\omega) \tag{B5}$$

to perform the integral in the limit as t goes to inifinity we arrive at Eq. (20).

[1] S. Inouye *et al.*, Nature (London) **392**, 151 (1998).
[2] E. Timmermans, P. Tommasini, M. Hussein, and A. Kerman, Phys. Rep. **315**, 199 (1999).
[3] P. O. Fedichev, Yu Kagan, G. V. Shlyapnikov, and J. T. M. Walraven, Phys. Rev. Lett. **77**, 2913 (1996).
[4] M. Theis, G. Thalhammer, K. Winkler, M. Hellwig, G. Ruff, R. Grimm, and J. H. Denschlag, Phys. Rev. Lett. **93**, 123001 (2004).
[5] R. Wynar *et al.*, Science **287**, 1016 (2000).
[6] E. A. Donley, N. R. Claussen, S. T. Thompson, and C. E. Wieman, Nature (London) **417**, 529 (2002).
[7] S. Dürr, T. Volz, A. Marte, and G. Rempe, Phys. Rev. Lett. **92**, 020406 (2004).
[8] M. Greiner, C. A. Regal, and D. S. Jin, Nature (London) **426**, 537 (2003).
[9] M. W. Zwierlein *et al.*, Phys. Rev. Lett. **91**, 250401 (2003).
[10] S. Jochim *et al.*, Science **301**, 2101 (2003).
[11] M. Greiner, O. Mandel, T. Esslinger, T. W. Hänsch, and I. Bloch, Nature (London) **415**, 39 (2002).
[12] M. Greiner, O. Mandel, T. W. Hänsch, and I. Bloch, Nature (London) **419**, 51 (2002).
[13] D. Jaksch, C. Bruder, J. I. Cirac, C. W. Gardiner, and P. Zoller, Phys. Rev. Lett. **81**, 3108 (1998).
[14] H. T. C. Stoff, *Condensed Matter Physics with Trapped Atomic Fermi Gases*, Course CXL, Proceedings of the International School of Physics "Enrico Fermi," Varenna, 1998 (IOS Press, Amsterdam, 1999).
[15] E. Timmermans, Phys. Scr. **T110**, 302 (2004).
[16] E. Timmermans, K. Furuya, P. W. Milonni, and A. K. Kerman, Phys. Lett. A **285**, 288 (2001).
[17] C. A. Regal, M. Greiner, and D. S. Jin, Phys. Rev. Lett. **92**, 040403 (2004).

[18] M. Bartenstein *et al.*, Phys. Rev. Lett. **92**, 120401 (2004).
[19] M. Zwierlein *et al.*, Phys. Rev. Lett. **92**, 120403 (2004).
[20] H. T. C. Stoof, M. Houbiers, C. A. Sackett, and R. G. Hulet, Phys. Rev. Lett. **76**, 10 (1996).
[21] G. Bruun, Y. Castin, R. Dum, and K. Burnett, Eur. Phys. J. D **7**, 433 (1999).
[22] C. Chin, M. Bartenstein, A. Altmeyer, S. Riedl, S. Jochim, J. Hecker Denschlag, and R. Grimm, Science **305**, 1128 (2004).
[23] J. Kinast, S. L. Hemmer, M. E. Gehm, A. Turlapov, and J. E. Thomas, Phys. Rev. Lett. **92**, 150402 (2004).
[24] M. Bartenstein, A. Altmeyer, S. Riedl, S. Jochim, C. Chin, J. H. Denschlag, and R. Grimm, Phys. Rev. Lett. **92**, 203201 (2004).
[25] E. A. Burt, R. W. Ghrist, C. J. Myatt, M. J. Holland, E. A. Cornell, and C. E. Wieman, Phys. Rev. Lett. **79**, 337 (1997).
[26] D. Hellweg, L. Cacciapuoti, M. Kottke, T. Schulte, K. Sengstock, W. Ertmer, and J. J. Arlt, Phys. Rev. Lett. **91**, 010406 (2003).
[27] L. Cacciapuoti, D. Hellweg, M. Kottke, T. Schulte, W. Ertmer, J. J. Arlt, K. Sengstock, and L. Santos, Phys. Rev. A **68**, 053612 (2003).
[28] E. Altman, E. Demler, and M. D. Lukin, Phys. Rev. A **70**, 013603 (2004).
[29] R. Bach and K. Rzażewski, Phys. Rev. Lett. **92**, 200401 (2004).
[30] R. J. Glauber, Phys. Rev. **130**, 2529 (1963).
[31] R. J. Glauber, Phys. Rev. **131**, 2766 (1963).
[32] M. Naraschewski and R. J. Glauber, Phys. Rev. A **59**, 4595 (1999).
[33] K. E. Cahill and R. J. Glauber, Phys. Rev. A **59**, 1538 (1999).
[34] D. Meiser and P. Meystre, Phys. Rev. Lett. **94**, 093001 (2005).
[35] M. Holland, S. J. J. M. F. Kokkelmans, M. L. Chiofalo, and R. Walser, Phys. Rev. Lett. **87**, 120406 (2001).
[36] M. L. Chiofalo, S. J. J. M. F. Kokkelmans, J. N. Milstein, and M. J. Holland, Phys. Rev. Lett. **88**, 090402 (2002).
[37] D. A. W. Hutchinson, E. Zaremba, and A. Griffin, Phys. Rev. Lett. **78**, 1842 (1997).
[38] J. Reidl, A. Csordás, R. Graham, and P. Szépfalusy, Phys. Rev. A **59**, 3816 (1999).
[39] T. Bergeman, D. L. Feder, N. L. Balazs, and B. I. Schneider, Phys. Rev. A **61**, 063605 (2000).
[40] D. A. Butts and D. S. Rokhsar, Phys. Rev. A **55**, 4346 (1997).
[41] M. Houbiers *et al.*, Phys. Rev. A **56**, 4864 (1997).
[42] E. Merzbacher, *Quantum Mechanics*, 3rd ed. (John Wiley & Sons, New York, 1998).